Journal of Applied Pharmaceutical Science Vol. 15(04), pp 116-128, April, 2025
Available online at http://www.japsonline.com
DOI: 10.7324/JAPS.2025.214803
ISSN 2231-3354

The potential of citral isomers from lemongrass (*Cymbopogon citratus*) essential oil as WAT browning agents in obesity by activating AMPK and PPARγ: An *in silico* approach

Musthika Wida Mashitah[1,2*], Nashi Widodo[3], Nur Permatasari[4], Achmad Rudijanto[5]

[1]Doctoral Program in Medical Science, Faculty of Medicine, Universitas Brawijaya, Malang, Indonesia.
[2]Department of Nursing, Faculty of Health Sciences, Institute of Technology, Science and Health, Dr. Soepraoen Hospital, Malang, Indonesia.
[3]Department of Biology, Faculty of Mathematics and Natural Science, Universitas Brawijaya, Malang, Indonesia.
[4]Department of Pharmacology, Faculty of Medicine, Universitas Brawijaya, Malang, Indonesia.
[5]Division of Endocrinology and Metabolic Disease, Department of Internal Medicine, Faculty of Medicine, Universitas Brawijaya, Dr. Saiful Anwar Hospital, Malang, Indonesia.

ARTICLE HISTORY

Received on: 28/08/2024
Accepted on: 06/02/2025
Available Online: 05/03/2025

Key words:
Anti-obesity, WAT browning, citral, PPARγ, AMPK.

ABSTRACT

Obesity is characterized by abnormal fat accumulation in the white adipose tissue (WAT), posing a significant health risk. Enhancing energy expenditure through WAT browning using dietary components and natural extracts is a promising therapeutic strategy for obesity management. This study explored the efficacy of citral isomers from *Cymbopogon citratus* (lemongrass) essential oil as agents for WAT browning by activating primarily the proliferator-activated receptor gamma (PPARγ) and AMPK, utilizing an *in silico* approach. Essentials oil were extracted from lemongrass leaves and stalks via steam-hydro distillation, and the citral isomer content was analyzed through gas chromatography-mass spectrophotometry. Molecular docking was performed using AutoDock Vina, and molecular dynamics simulations were conducted using YASARA. Five citral isomers were identified: geranial, neral, geranial diethyl acetal (GDA), isogeranial, and isoneral isomers. This study identified GDA and neral as the most effective AMPK agonists, acting by directly activating their allosteric sites. Additionally, GDA, isoneral, and neral demonstrate PPARγ agonist properties by stabilising the protein's active site. In conclusion, citral isomers in lemongrass essential oil hold the potential to act as WAT browning agents in obesity management through the activation of AMPK and PPARγ. Future *in vitro* and *in vivo* studies are required to validate these findings.

INTRODUCTION

Obesity is one of the most pressing health concerns worldwide. The prevalence of obesity has dramatically increased worldwide over the last four decades, with predictions indicating that the majority of the world's adult population will be overweight or obese by 2030 [1]. Obesity is classified as a chronic, non-communicable disease that poses significant risks for the development of other chronic diseases such as cardiovascular disease and diabetes mellitus [2]. Obesity is characterized by abnormal fat accumulation, which poses significant health risks [3]. This condition arises when energy intake consistently exceeds energy expenditure, leading to the storage of excess energy, primarily as triglycerides in white adipose tissue (WAT) [4]. The expansion of adipose tissue in obesity results in adipocyte hypertrophy, triggering a cascade of inflammatory responses within the tissue. This inflammation is marked by enhanced lipolysis, the production of proinflammatory cytokines and chemokines, and the secretion of free fatty acids into the circulation. The release of chemokines that facilitate the recruitment of macrophages from the bloodstream, thereby increasing their infiltration and exacerbating inflammation, which is further compounded by

*Corresponding Author
Musthika Wida Mashitah, Doctoral Program in Medical Science, Faculty of Medicine, Universitas Brawijaya, Malang, Indonesia.
Email: ns.musthika @ itsk-soepraoen.ac.id

elevated levels of proinflammatory cytokines such as tumor necrosis factor α and interleukin-6 (IL-6). Additionally, the dysregulation of adipokine secretion—including leptin, adiponectin, and resistin—contributes to this inflammatory state. These adipokines, whether derived from macrophages or adipose tissue, operate in a paracrine or autocrine manner, intensifying the inflammatory response in the adipose tissue. Systemically, alterations in adipokine secretion can lead to decreased insulin sensitivity in skeletal muscles and the liver, primarily because of increased ectopic lipid deposition and persistent inflammation [5,6].

Current recommended therapies for obesity are supported by evidence-based research, including lifestyle interventions, pharmacotherapy, and bariatric surgery [7]. Although lifestyle-based programs typically result in approximately 10% weight loss, the challenge of preventing weight regain remains significant [8,9]. Most patients regain approximately 30% of their lost weight within 1 year and often return to their original weight within 3–5 years [9]. As lifestyle and behavioral interventions demonstrate only moderate effectiveness, it is essential to enhance obesity treatment strategies by incorporating pharmacological or surgical interventions. However, surgical interventions alone are insufficient to address the global medical demand. Achieving long-term weight normalization through pharmacotherapy while ensuring tolerability and safety remains a formidable challenge [10].

The adipose tissue in mammals comprises WAT and brown adipose tissue (BAT). WAT serves primarily as a lipid store, whereas BAT oxidizes lipids to fuel thermogenesis by expressing uncoupling protein-1 (UCP-1) [4,11,12]. Recent studies have demonstrated that increased WAT browning has significant therapeutic potential for treating obesity and associated metabolic disorders [13–15]. White adipocytes can be transformed into brown-like adipocytes or beige adipocytes in response to various stimuli, including chronic exposure to cold temperatures, physical exercise, nutrition, and pharmaceutical agents (e.g., PPARγ, β3-AR, and AMPK agonists) [16–18]. WAT browning promotes lipid oxidation, increases energy expenditure, and reducing adiposity [19].

These white-to-beige transformations increase mitochondrial content and induce the expression of UCP-1, a thermogenic protein that boosts energy expenditure following stimulation [16,20,21]. UCP-1 expression in beige adipocytes is regulated by several transcription factors, primarily the proliferator-activated receptor gamma (PPARγ). In addition to transcription factors, coactivators such as the proliferator-activated receptor-gamma coactivator 1 α and positive regulatory domain zinc finger region protein 16 (PRDM16) play essential roles. PPARγ recruits PRDM16 to form a core transcription complex that differentiates beige adipocytes from white adipocytes. This complex also recruits PGC1α, enhancing the thermogenic capacity and mitochondrial biogenesis in beige adipocytes [13,16,20,22,23]. Another browning pathway involves the activation of AMP-activated protein kinase (AMPK), which activates Sirtuin-1 (SIRT1), leading to deacetylation and enhanced interaction between PPARγ/PRDM16/PGC1α. Furthermore, AMPK can amplify PGC1α activity through phosphorylation, thereby fostering mitochondrial biogenesis [13,16,20,22–25].

Despite advances in understanding the developmental lineages and transcription factors that regulate brown and beige adipocytes, the role of environmental modifiers, such as dietary components and natural extracts, remains to be elucidated. Furthermore, the undesirable pleiotropic effects associated with synthetic drugs targeting adipose tissue browning and thermogenesis highlight the need for research on alternative natural sources to combat obesity and related metabolic disorders [16].

Lemongrass (*Cymbopogon citratus)* has gained attention because of the commercial value of its essential oil, which is widely utilized in food technology and traditional medicine. Lemongrass has also been shown to help reduce uric acid, cholesterol, blood pressure, and excess fat while stimulating digestion, blood circulation, and lactation [26]. An analysis of lemongrass essential oil, obtained through hydro-distillation and characterized using gas chromatography-mass spectrophotometry (GC-MS), revealed that citral (a blend of neral and geranial) constitutes the primary component [27,28].

Citral has been shown to function as a PPARγ agonist [29,30]. When activated by citral, PPARγ can therapeutically address metabolic syndrome and lifestyle-related diseases [29–31]. PPARγ agonists are potent regulators of the browning process. PPARγ agonists are considered potential agents for inducing browning in adipose tissue [32,33].

Administration of lemongrass ethanol extract to 3T3-L1 preadipocyte cultures significantly increased AMPK activity [34]. Following this activation, AMPK can activate SIRT1, following this activation, leading to the deacetylation and enhanced interaction with the PPARγ/PRDM16/PGC1α complex. Moreover, AMPK can also directly improve the PGC1α activity [13,16,25], illustrating that lemongrass essential oil, particularly its citral content, has the potential to act as a browning agent through the activation of both PPARγ and AMPK pathways. However, the effectiveness of citral as a browning agent has not yet been extensively explored in research. This study aimed to evaluate the citral content and its isomers in the essential oil of lemongrass leaves and stalks using GC-MS and computational analysis to examine its potential as a browning agent for WAT via the AMPK and PPARγ pathways. This study represents the first comprehensive interaction analysis of the interaction of all five citral isomers in lemongrass with AMPK and PPARγ.

MATERIALS AND METHODS

Plant material

Cymbopogon citratus was sourced from local lemongrass farmers in Wagir, Malang Regency, East Java, Indonesia (-9°59’4.51”N, 112°32’52.93”W). The species was authenticated as *Cymbopogon citratus* by Balai Materia Medica Laboratory in Batu, East Java, Indonesia, under determination number 067/1957/102.20/2023. Following harvesting, the lemongrass was thoroughly cleaned, and the leaves and the stalks were separated and then cut into small pieces ranging from 4 to 8 mm for distillation in their fresh form.

Table 1. Active side residues in the binding pocket area and grid box coordinates for specific docking.

Protein	PDB ID	Active site	Grid box coordinate (A)		References
			Center	Dimension	
AMPK	4CFF	Val11; Leu18; Lys29; Lys31; Ile46; Asn48; Val81; Arg83; Asp88; Phe90; Thr106; Arg107; Asn111; Val113; Ile115	X: -23.5676	X: 21.0932	[35]
			Y: -9.2633	Y: 22.3059	
			Z: 205.0694	Z: 23.4946	
PPARG	1FM6	Phe282; Gly284; Cys285; Gln286; Arg288; Ser289; His323; Ile326; Tyr327; Leu330; Leu333; Val339; Leu340; Ile341; Ser342; Met364; His449; Leu453; Leu465; Leu469; Tyr473	X: 17.6241	X: 27.9639	[36]
			Y: -17.4264	Y: 24.7435	
			Z: 11.2950	Z: 25.0544	

Table 2. Compounds of essential oils of lemongrass leaves and stalks.

No.	Name of compound	Molecular formula	Molecular weight	Lemongrass leaves		Lemongrass stalks	
				RT	%A	RT	%A
1	Geranial*	$C_{10}H_{16}O$	152	15.91	34.86	16.14	24.25
2	Neral*	$C_{10}H_{16}O$	152	15.02	28.49	15.23	19.36
3	β-Pinene	$C_{10}H_{16}$	136	7.89	12.01	7.91	3.02
4	Geranial diethyl acetal*	$C_{14}H_{26}O_2$	226	19.73	10.28	20.35	17.84
5	Isogeranial*	$C_{10}H_{16}O$	152	13.37	1.81	13.37	1.29
6	Isoneral*	$C_{10}H_{16}O$	152	12.86	1.28	12.85	0.83
7	5,5-Dimethyl-1-vinylbicyclo[2.1.1]hexane	$C_{10}H_{16}$	136	7.87	1.19	–	–
8	Linalool	$C_{10}H_{18}O$	154	11.03	1.10	11.02	0.72
9	Geraniol	$C_{10}H_{18}O$	154	15.59	0.92	15.72	0.94
10	Ethyl iso-allocholate	$C_{26}H_{44}O_5$	436	34.80	0.88	49.33	0.19
11	ß-Ocimene	$C_{10}H_{16}$	136	9.21	0.56	9.21	0.58
12	1-Heptatriacotanol	$C_{37}H_{76}O$	536	21.07	0.52	34.52	0.36
13	Selin-6-en-4a-ol	$C_{15}H_{26}O$	222	24.56	0.51	24.59	8.95
14	Geranyl acetate	$C_{12}H_{20}O_2$	196	18.90	0.46	–	–
15	7-epi-cis-sesquisabinene hydrate	$C_{15}H_{26}O$	222	18.74	0.42	18.39	0.14
16	Citronellal	$C_{10}H_{18}O$	154	12.51	0.41	12.51	0.43
17	trans-Chrysanthemal	$C_{10}H_{16}O$	152	12.38	0.38	–	–
18	9-Desoxo-9-x-acetoxy-3,8,12-tri-O-acetylingol	$C_{28}H_{40}O_{10}$	536	51.60	0.29	–	–
19	Linalool formate	$C_{11}H_{18}O_2$	182	19.03	0.29	–	–
20	6-Methyl-4,6-bis(4-methylpent-3-en-1-yl) cyclohexa-1,3-dienecarbaldehyde	$C_{20}H_{30}O$	286	34.51	0.28	–	–
21	Cyclopropanemethanol, 2-methyl-2-(4-methyl-3-pentenyl)-	$C_{11}H_{20}O$	168	13.72	0.26	–	–
22	Patchouli alcohol	$C_{15}H_{26}O$	222	25.44	0.26	–	–
23	2-Pentadecyn-1-ol	$C_{15}H_{28}O$	224	10.65	0.19	–	–
24	cis-a-Bergamotene	$C_{15}H_{24}$	204	20.14	0.15	–	–
25	α-Cadinol	$C_{15}H_{26}O$	222	25.37	0.13	25.47	3.41
26	2-Isopropenyl-5-methylhex-4-enal	$C_{10}H_{16}O$	152	16.56	0.12	17.33	0.11
27	1-Pentanol, 5-(methylenecyclopropyl)-	$C_9H_{16}O$	140	10.80	0.12	–	–
28	Isochavibetol	$C_{10}H_{12}O_2$	164	18.42	0.11	–	–
29	1-Undecyne	$C_{11}H_{20}$	152	12.08	0.10	–	–
30	T-Muurolol	C15H26O	222	–	–	25.16	2.02
31	Intermedeol	C15H26O	222	–	–	25.53	1.82
32	a-epi-7-epi-5-Eudesmol	C15H26O	222	–	–	24.32	1.62

Continued

No.	Name of compound	Molecular formula	Molecular weight	Lemongrass leaves		Lemongrass stalks	
				RT	%A	RT	%A
33	1-Naphthalenol, decahydro-1,4a-dimethyl-7-(1-methylethylidene)-, [1R-(1a,4aß,8aa)]-	C15H26O	222	–	–	26.34	1.50
34	Kusenol	C15H26O	222	–	–	24.97	1.36
35	Germacrene D-4-ol	C15H26O	222	–	–	23.58	1.03
36	a-acorenol	C15H26O	222	–	–	25.71	0.65
37	Kessane	C15H26O	222	–	–	28.87	0.61
38	Cadina-1(10),4-diene	C15H24	204	–	–	22.31	0.58
39	3,7-Cyclodecadiene-1-methanol, a,a,4,8-tetramethyl-, [s-(Z,Z)]	C15H26O	222	–	–	22.96	0.47
40	2-Naphthalenemethanol, decahydro-a,a,4a-trimethyl-8-methylene-, [2R-(2a,4aa,8aß)]-	C15H26O	222	–	–	25.34	0.45
41	3-Buten-2-one, 3-methyl-4-(1,3,3-trimethyl-7-oxabicyclo[4.1.0]heptan-1-yl)-	C14H22O2	222	–	–	28.99	0.43
42	1-Naphthalenol, 1,2,3,4,4a,7,8,8a-octahydro-1,6-dimethyl-4-(1-methylethyl)-, [1R-(1a,4ß,4aß,8aß)]-	C15H26O	222	–	–	25.23	0.42
43	Cyclohexane, 1-ethenyl-1-methyl-2,4-bis(1-methylethenyl)-, [1S-(1a,2ß,4ß)]-	C15H24	204	–	–	19.04	0.31
44	2,6-Octadien-1-ol, 2,7-dimethyl-	C10H18O	154	–	–	8.22	0.29
45	Cis-beta-Copaene	C15H24	204	–	–	21.31	0.29
46	Froggatt ether/4-Epi-cis-Dihydroagarofuran	C15H26O	222	–	–	21.86	0.25
47	2,5,5,8a-Tetramethyl-4-methylene-6,7,8,8a-tetrahydro-4H,5H-chromen-4a-yl hydroperoxide	C14H22O3	238	–	–	29.22	0.23
48	6-Octenal, 7-methyl-3-methylene-	C10H16O	152	–	–	12.29	0.23
49	Epiglobulol	C15H26O	222	-	–	25.91	0.22
50	Geranyl vinyl ether	C12H20O	180	-	–	18.92	0.19
51	(3S,3aR,3bR,4S,7R,7aR)-4-Isopropyl-3,7-dimethyloctahydro-1H-cyclopenta[1,3]cyclopropa[1,2]benzen-3-ol	C15H26O	222	–	–	22.16	0.18
52	9-Desoxo-9-x-acetoxy-3,8,12-tri-O-acetylingol	C28H40O10	536	–	–	51.59	0.15
53	a-Muurolene	C15H24	204	–	–	21.75	0.15
54	Muurolene	C15H24	204	–	–	22.08	0.15
55	Shyobunol	C15H26O	222	–	–	27.07	0.14
56	Methyl heptenone	C8H14O	126	–	–	7.80	0.13
57	Eucalyptol	C10H18O	154	–	–	8.97	0.13
58	(3R,3aR,3bR,4S,7R,7aR)-4-Isopropyl-3,7-dimethyloctahydro-1H-cyclopenta[1,3]cyclopropa[1,2]benzen-3-ol	C15H26O	222	–	–	21.65	0.12
59	Caryophyllene oxide	C15H24O	220	–	–	23.72	0.11

*: citral isomers; RT: retention times; %A: peak area.

Extraction

The lemongrass essential oil was extracted using steam-hydrodistillation. The distillation kettle was filled with water up to 5 cm below the filter level. The raw material was then placed in the filter, and water-vapor-carrying essential oil particles flowed through the pipe to the cooler, where the vapor condensed, allowing the essential oil to liquefy. The resulting essential oil was collected in a separator to distinguish it from water. An essential oil distillation apparatus with a capacity of 3 kg to conduct the distillation over 4 hours at a temperature of approximately 100°C. The essential oil obtained from the lemongrass leaves and stalks was stored in a sealed glass bottle at room temperature and shielded from direct sunlight.

Gas chromatography-mass spectrometry

The GC-MS analysis of the essential oil derived from lemongrass leaves and stalks was conducted using a Thermo Scientific™ TRACE 1310 GC coupled with a Thermo Scientific™ ISQ LT Single Quadrupole Mass Spectrometer with an HP-5MS UI column (30 m × 0.25 mm × 0.25 µm) (5%-diphenyl, 95% dimethyl polysiloxane). GC-grade helium was utilized as a carrier gas at a 1 ml/minute flow rate, and 1 µl splitless injection was employed. The injector temperature was maintained at 300°C, and the source temperature was 250°C. The oven temperature was initially set to 50°C and held for 2 minutes, then ramped to 280°C at 5°C/minute, maintained this temperature for 5 minutes. The identification and calculation of

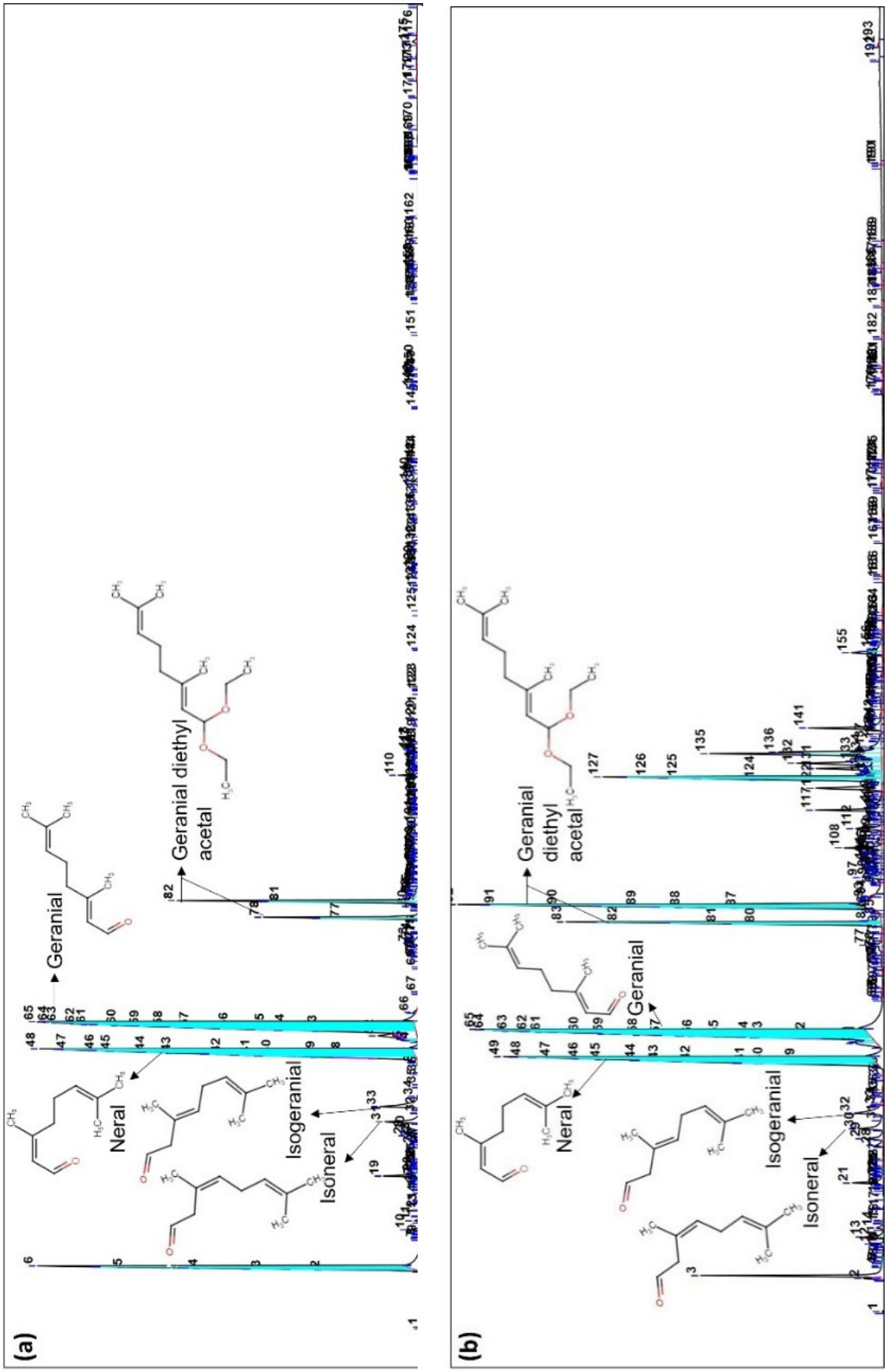

Figure 1. GC-MS spectrum of essential oils of lemongrass leaves (a) and stalks (b).

the relative percentage of each component in the lemongrass essential oil were determined using the Thermo Fisher Scientific Chromeleon 7 software library.

Ligand preparation

The 3D structures of citral isomers, the AMPK agonist (cordycepin), and the PPARγ agonist (rosiglitazone) used as a control were retrieved from the PubChem database (https://pubchem.ncbi.nlm.nih.gov/). The compound molecules were prepared for energy minimization using OpenBabel in PyRx 0.8 software.

Table 3. Binding affinity values of each compound that binds to AMPK and PPARγ.

Compound	PDB ID/ PubChem ID	Binding affinity (kcal/mol)	
		AMPK	PPARγ
Cordycepin (AMPK Control)	6303	−7.0	–
Rosiglitazone (PPARγ Control)	1FM6	–	−8.5
Geranial diethyl acetal (GDA)	5365794	−5.8	−5.5
Geranial	638011	−5.2	−5.3
Isogeranial	6428928	−5.2	−5.2
Isoneral	20837773	−5.1	−5.6
Neral	643779	−5.1	−5.4

Protein preparation

The 3D structures of the target proteins AMPK (PDB ID: 4CFF) and PPARγ (PDB ID: 1FM6) were retrieved from the RCSB PDB database (https://www.rcsb.org/). Each protein was prepared by removing unnecessary molecules or atoms in preparation for the molecular docking process using the PyMol ver 2.6 software.

Molecular docking

Molecular docking was performed by targeting specific docking sites on the grid box and binding pocket of each protein using AutoDock Vina integrated into PyR× 0.8. The active site of the protein and coordinates of the grid box of the molecular docking area are listed in Table 1 [35,36]. The Molecular docking results were subsequently analyzed to compare the binding affinity values of each complex against the control compound for each protein, expressed in kcal/mol. Compounds demonstrating the best binding affinity were

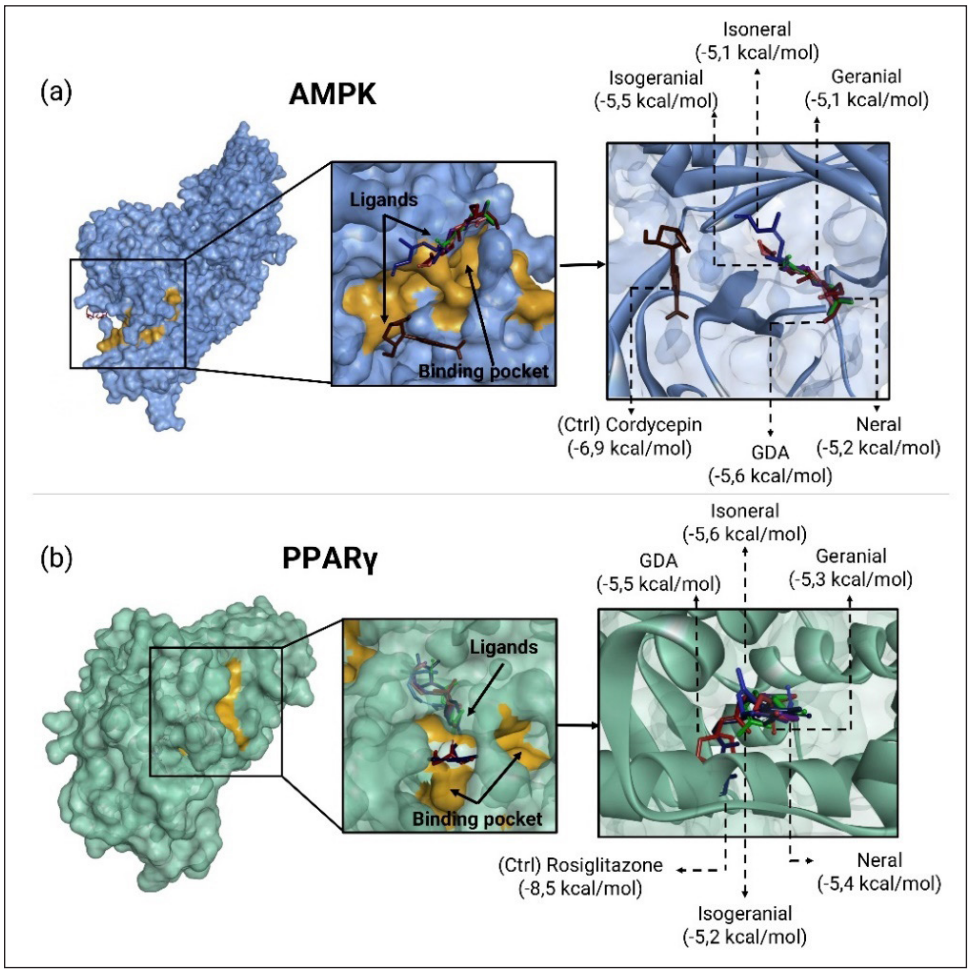

Figure 2. Binding pocket and binding pose of (a) AMPK protein and (b) PPARγ protein.

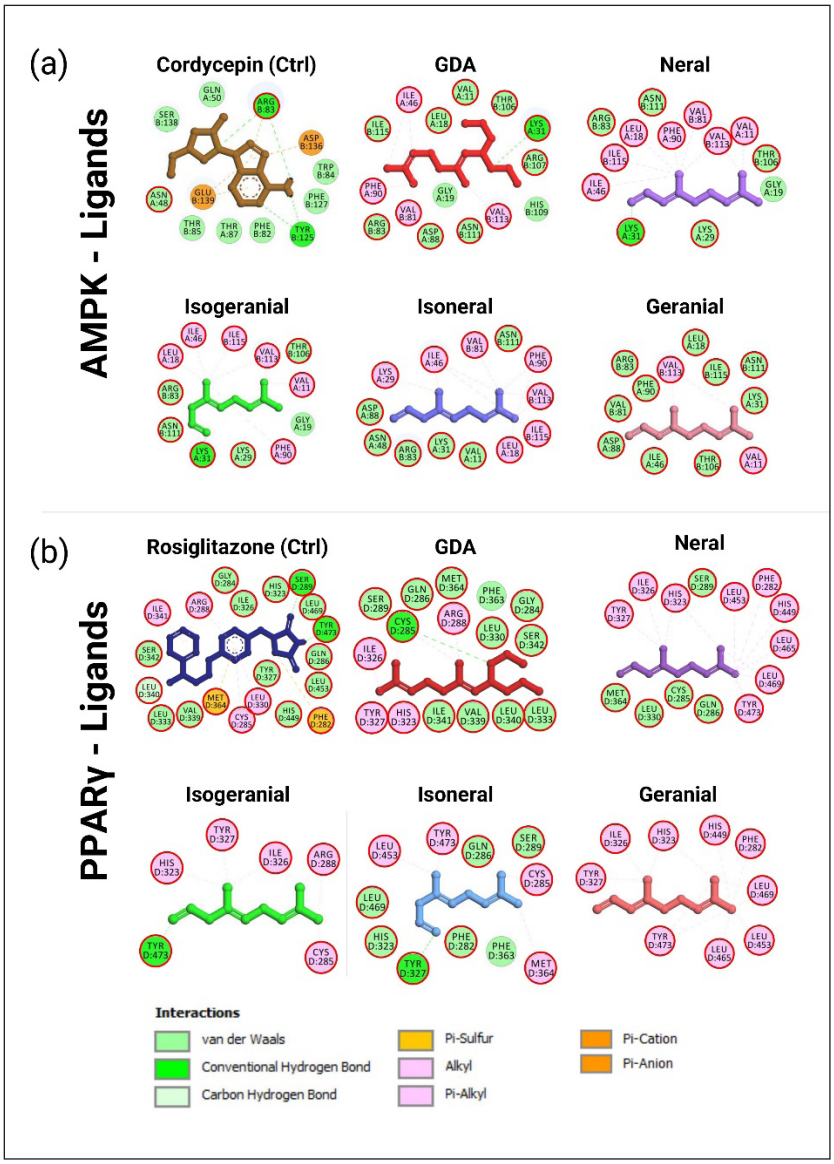

Figure 3. Visualization of lemongrass essential oil compound structure and interactions involved in molecular docking results with (a) AMPK and (b) PPARγ proteins. The red circle indicated the same amino acid residue in the active sites.

selected and visualized using Biovia Discovery Studio 2019 to analyze their interactions and optimal binding positions within the binding pocket [37].

Molecular dynamics

The interactions between the compounds and protein complexes exhibiting the highest binding affinity from molecular docking were further investigated to assess binding using molecular dynamics simulations. This simulation employed YASARA (Yet Another Scientific Artificial Reality Application) software, utilizing a modified AMBER14 force field [38]. Each complex was simulated for 20 ns under conditions mimicking cellular physiology (temperature 310K, pH 7.4, pressure 1 atm, and 0.9% NaCl) for 20 ns. The macro program utilized included md_runfast to start the simulation, md_analyze to analyze the root mean square deviation (RMSD) results, and md_analyzerez to evaluate the root mean square fluctuation (RMSF) results.

RESULTS

Compounds in essential oils of lemongrass leaves and stalks

The pale-yellow essential oils obtained from lemongrass leaves and stalks via steam distillation yielded 0.28% and 0.27%, respectively. A total of 67 compounds were identified in the leaves, whereas 80 compounds were identified in the oil from the stalks, potentially contributing to their medicinal properties. The percentage values of the compounds in the essential oils of lemongrass leaves and stalks are presented in Table 2, and their corresponding spectral peaks are shown in Figure 1.

Table 4. List of chemical interactions on protein amino acid residues.

Protein	Ligand	Position of chemical bonds	
		Hydrogen bond	Hydrophobic interaction
AMPK	Cordycepin (Control)	B: **Arg83**; Tyr125	–
	GDA	A: **Lys 31**	A: **Ile46; Phe90**
			B: **Val81; Val 113**
	Isogeranial	A: **Lys 31**	A: **Val11; Leu18; Ile46, Phe90**
			B: **Val113; Ile115**
	Neral	A: **Lys 31**	A: **Val11; Leu18; Ile46, Phe90**
			B: **Val81; Val113; Ile115**
	Isoneral	–	A: **Leu18; Lys29; Ile46; Phe90**
			B: **Val81; Val113, Ile115**
	Geranial	–	A: **Val11**
			B: **Val113**
PPARγ	Rosiglitazone (Control)	D: **Ser289; Leu340; Tyr473**	D: **Cys285; Arg288; Leu330; Ile341**
	GDA	D: **Cys285**	D: **Arg288; His323; Ile326; Tyr327**
	Isoneral	D: **Tyr327**	D: **Cys285; Leu453; Met364; Tyr473**
	Neral	–	D: **Phe282; His323; Ile326; Tyr327; His449; Leu453; Leu465; Leu469; Tyr473**
	Geranial	–	D: **Phe282; His323; Ile326; Tyr327; His449; Leu453; Leu465; Leu469; Tyr473**
	Isogeranial	D: **Tyr473**	D: **Cys285; Arg288; His323; Ile326; Try327**

Bold: Chemical interaction at the same residue as the control compound or active side of the protein
A/B/D: Protein chain.

Five isomers of citral were identified: geranial, neral, geranial diethyl acetal (GDA), isogeranial, and isoneral. The dominant compounds were geranial (trans-citral) and neral (cis-citral), with citral accounting for 63.35% of the total composition (comprising 34.86% geranial and 28.49% neral). The essential oil from the leaves contained 10.28% GDA, 1.81% isogeranial, and 1.28% isoneral. In contrast, the essential oil from lemongrass stalks showed that citral accounted for 43.60% citral (24.25% geranial and 19.36% neral), 17.84% GDA, 1.29% isogeranial, and 0.83% isoneral).

Interaction of citral isomers with AMPK and PPARγ proteins

Molecular docking analysis of citral isomers with AMPK and PPARγ revealed diverse results (Table 3). The docking of AMPK with the five citral isomers demonstrated varying binding affinities, ranked from the lowest to highest as follows: GDA at −5.8 kcal/mol, geranial at −5.2 kcal/mol, isogeranial at −5.2 kcal/mol, isoneral at −5.1 kcal/mol, and neral at −5.1 kcal/mol. In the case of PPARγ, the binding affinities for the citral isomers were also ranked from lowest to highest: at −5.6 kcal/mol, GDA at −5.5 kcal/mol, neral at −5.4 kcal/mol, geranial at −5.3 kcal/mol, and isogeranial at −5.2 kcal/mol. Although the binding affinity values of all compounds were lower than those of the control compounds with the AMPK agonist cordycepin at −7.0 kcal/mol and the PPARγ agonist rosiglitazone at −8.5 kcal/mol, all compounds demonstrated similar binding sites in the binding pocket of AMPK and PPARγ (Fig. 2).

Based on the analysis of the chemical interactions shown in Figure 3 and Table 4, most compounds interacted with identical amino acid residues as the active site residues and control compounds. GDA, isogeranial, and neral formed the same hydrogen bond at Lys31 along with several hydrophobic interactions with the active site residues of AMPK. In contrast, isoneral and geranial did not form hydrogen bonds but were supported by multiple hydrophobic interactions. GDA, isoneral, and isogeranial interaction with PPARγ also involved interactions with most of the residues in the binding pocket. Specifically, GDA forms hydrogen bonds at Cys285, isoneral at Tyr327, and isogeranial at Tyr473. In contrast, neral and geranial did not form hydrogen bonds but exhibited higher hydrophobic bonds than GDA, isoneral, and isogeranial.

Molecular dynamics

The RMSD backbone simulations of AMPK with all compounds indicated that geranial and neral demonstrated relatively good stability. Other compounds, including cordycepin and isoneral, exhibited high fluctuations with RMSD values exceeding 3Å. The RMSD Ligand Movement showed good stability for the neral, with cordycepin being the most unstable ligand. The RMSF graph for AMPK protein showed similar fluctuations during simulations with all ligands, particularly in residues Glu295, Gln145, and Cys173 (Fig. 4a).

The results of the molecular dynamics simulations of PPARγ are illustrated in Figure 4b**,** demonstrating relatively more stable protein-ligand interactions. The backbone protein RMSD graph indicated the stability of the protein when interacting with all compounds. The RMSD Ligand Movement analysis showed minor fluctuations with isoneral and geranial, while the other compounds did not exhibit significant movement.

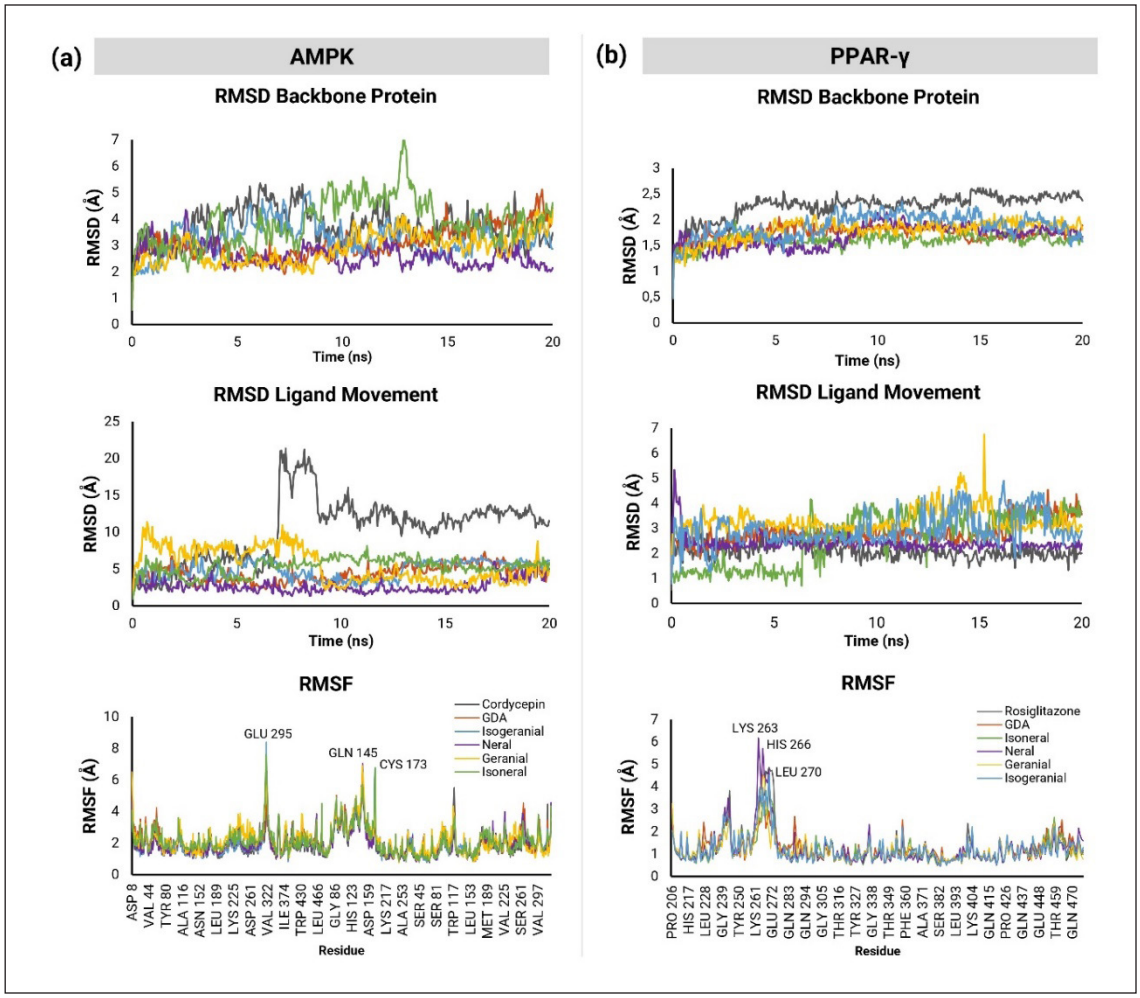

Figure 4. Molecular dynamics of protein (RMSD Backbone Protein), ligand (RMSD Ligand Movement), and stability of a) AMPK and b) PPARγ amino acid residues during simulation.

Specific amino acid residues, such as Lys263, His266, and Leu270, showed fluctuations in the RMSF graph but stabilized toward the end of the simulation.

DISCUSSION

The yields of lemongrass essential oil in this study were consistent with previous research, which indicated that lemongrass leaves typically contain essential oil concentrations ranging from 0.2% to 1.4% and can reach up to 3% [39]. Another study reported that the oil content in regular cuts should average 0.25%–0.50%, but with optimal management, it can reach 0.66%–0.90% [28]. The chemical composition of lemongrass essential oil varies depending on several factors, including geographic region, genetic differences, the plant part extracted, age of maturity, harvest season, drying method, and plant health status [40–43]. The findings align with those of previous research, which noted that the chemical composition of essential oils in lemongrass stalks is more significant than that in leaves [44–46].

In molecular docking, the binding affinity between a ligand and protein is defined as the average binding free energy in the conformation of all molecules in the molecular complex. A lower binding affinity value indicates a greater ease of interaction between the molecule and the protein [47]. While a low binding affinity in molecular docking can suggest limited interaction with proteins, it does not necessarily indicate a complete lack of interaction. The structural characteristics of citral compounds and their binding sites on proteins can significantly influence their interaction [48]. Further research is required to investigate the targeting mechanisms of citral compounds in the upstream and downstream pathways beyond AMPK and PPARγ.

The chemical bonds and interactions between compounds and proteins contributed to the stability of these interactions. Several types of interactions are involved, including hydrogen bonds, hydrophobic bonds, and van der Waals interactions [49]. The binding sites of all compounds were more proximal to the active site area than that of the control compound, cordycepin, suggesting the potential of these compounds as potent agonists of AMPK. Binding sites were also similar to the control PPARγ agonist, rosiglitazone, in the binding pocket, indicating the potential of these compounds to activate PPARγ. These interactions strongly supported the

stability of compound interactions with AMPK and PPARγ [50].

This research is supported by previous studies showing that the administration of citral suppresses lipogenesis in prostate cancer cells through the activation of AMPK phosphorylation [51], and that the administration of anethanol extract of lemongrass in 3T3-L1 preadipocyte cultures increases AMPK activity [34]. Citral inhibits lipopolysaccharide-induced acute lung injury by activating PPARγ both *in vitro* and *in vivo* [30]. As a lemongrass oil component, citral activated PPARγ in cell-based transfection assays, potentially offering therapeutic benefits for addressing metabolic syndrome and lifestyle-related diseases [29].

The interaction of all compounds with the active site of AMPK suggests potential agonistic activity, as they bind near the cordycepin-binding area in the AMPK-binding pocket. AMPK is a heterodimer complex comprising α-catalytic subunits and β- and γ- regulatory subunits [52]. Three mechanisms of AMPK activation by activator molecules have been identified: indirect activation by increasing intracellular AMP and ADP levels, direct activation by binding to the allosteric binding site, and activation that mimics the character of AMP or ATP for binding to the γ-subunit [53].

Cordycepin, a bioactive compound from *Cordyceps militaris*, was used as a control compound because of its ability to activate AMPK by acting as an AMP analogue in the form of cordycepin monophosphate, which binds to the γ1-subunit [54]. The structure of the compounds in lemongrass essential oil presented marked variations and conformations compared to cordycepin, as evidenced by the difference in binding sites between the compounds and cordycepin (Fig. 3). Most of the compounds could bind specifically to the allosteric drug and metabolite (ADaM) site of AMPK. The ADaM site is located between the kinase domain of the α-subunit and the carbohydrate binding module on the β-subunit [55]. Direct activation at this site can enhance AMPK via allosteric kinase or prevent dephosphorylation at Thr-172, thus inhibiting AMPK inactivation [56]. Therefore, the binding of these compounds to the ADaM site has the potential to exert an agonistic effect on AMPK.

As a critical regulator of the adipocyte browning process, AMPK plays a vital role in modulating adipogenesis by inhibiting the mammalian target of the rapamycin signaling pathway, demethylation of PRDM16, and activation of PPARγ [57]. Several signaling cascades, including PGC1α, PPARγ, mitochondrial fission factor, and unc-51-like autophagy activating kinase 1, contribute to white adipocytes' browning process [58,59].

The binding affinity values and specific binding residues of each compound in lemongrass essential oil support the potential PPARγ agonist activities of most compounds. Rosiglitazone, a control compound, belongs to the thiazolidinediones, a group of antidiabetic agents that function as PPARγ agonist ligands [60]. PPARγ is a type II nuclear receptor that functions as a transcription factor [61]. The activation of PPARγ by rosiglitazone involves several critical amino acid residues, including Ser289, His323, His449, and Tyr473, which form hydrogen bonds [62]. The interactions formed by most compounds had identical binding residues as rosiglitazone, suggesting a similar PPARγ agonist activity. PPARγ and CCAAT-enhancer-binding proteins alpha (C/EBP-α) are essential for adipogenic differentiation and are expressed in mature adipocytes at the late adipogenic stage [63,64]. In 3T3-L1 fibroblast cells, the expression of the transcription factors PPARγ and C/EBP-α was also shown to be involved in the regulation of adipogenic-related genes [65]. PPARγ agonists may enhance the stabilization of PRDM16 protein, recruit PRDM16 to gene targets of PPARγ, increase its formation, and strengthen the PRDM16-PPARγ complex, thereby maintaining thermogenic capacity in beige adipocytes [32,33,66]. Activation of the complex modulates the expression of early B-cell factor and UCP-1, both crucial for the adipocyte browning process [67].

Molecular dynamics simulations of each complex were analyzed using parameters such as the RMSD Backbone Protein, RMSD Ligand Movement, and RMSF. The RMSD backbone protein indicated protein stability, while RMSD ligand movement represented the stability of ligands during simulation. RMSF measures the fluctuation stability of each amino acid residue throughout the simulation [68]. An RMSD value is considered stable if it does not exceed 3Å [38,69]. Elevated RMSF values at specific residues indicate instability of the corresponding amino acid during the interaction [70]. The molecular dynamics results suggested that GDA and neral were potentially more effective agonists and exhibited more excellent stability than cordycepin, which served as a control. Based on all the parameters assessed, the interaction of these compounds with PPARγ demonstrated good stability, indicating that they could function as competitive agonists alongside existing activator compounds, including rosiglitazone.

CONCLUSION

The citral content and its isomers in lemongrass essential oil have demonstrated potential as browning agents of WAT in obesity management through the activation of AMPK and PPARγ. GDA and neral emerged as the most potentially stable compounds acting as AMPK agonists by directly activating their allosteric sites. Additionally, GDA, isoneral, and neral exhibited characteristics indicative of PPARγ agonists by stabilizing their binding to the protein's active site of the protein. This research establishes a foundation for further *in vitro* and *in vivo* studies to validate these effects.

ACKNOWLEDGMENTS

The authors are grateful to Nuraini Rosyadah for assisting with the molecular dynamics simulation.

AUTHOR CONTRIBUTIONS

All authors made substantial contributions to the conception and design, acquisition of data, or analysis and interpretation of data; took part in drafting the article or revising it critically for important intellectual content; agreed to submit to the current journal; gave final approval of the version to be published; and agreed to be accountable for

all aspects of the work. All authors are eligible to be authors of the International Committee of Medical Journal Editors requirements/guidelines.

FINANCIAL SUPPORT

This research was funded by the Indonesian Endowment Funds for Education (LPDP-Lembaga Pengelola Dana Pendidikan), Ministry of Finance of the Republic of Indonesia, through a Lecturer-Educator Scholarship (SKPB-7063/LPDP/LPDP.3/2023).

CONFLICTS OF INTEREST

All the authors declare that there are no conflicts of interest.

ETHICAL APPROVALS

This study does not involve experiments on animals or human subjects.

DATA AVAILABILITY

All data generated and analyzed during this study are included in this research article.

PUBLISHER'S NOTE

All claims expressed in this article are solely those of the authors and do not necessarily represent those of the publisher, the editors and the reviewers. This journal remains neutral with regard to jurisdictional claims in published institutional affiliation.

USE OF ARTIFICIAL INTELLIGENCE (AI)-ASSISTED TECHNOLOGY

The authors declares that they have not used artificial intelligence (AI)-tools for writing and editing of the manuscript, and no images were manipulated using AI.

REFERENCES

1. Haththotuwa RN, Wijeyaratne CN, Senarath U. Chapter 1. Worldwide epidemic of obesity. Obesity and Obstetrics. New Delhi, India: INC; 2016. p 1–8. doi: https://dx.doi.org/10.1016/B978-0-12-817921-5.00001-1
2. Purnell JQ. Definitions, classification, and epidemiology of obesity—endotext—NCBI Bookshelf. South Dartmouth, MA: MDText.com, Inc; 2018. 22–8 pp.
3. WHO. Obesity and overweight. Geneva, Switzerland: WHO; 2021. Available from: https://www.who.int/news-room/fact-sheets/detail/obesity-and-overweight.
4. Jakab J, Miškić B, Mikšić Š, Juranić B, Ćosić V, Schwarz D, *et al.* Adipogenesis as a potential anti-obesity target: a review of pharmacological treatment and natural products. Diabetes, Metab Syndr Obes Targets Ther. 2021;14:67–83. doi: https://doi.org/10.2147/DMSO.S281186
5. Coelho M, Oliveira T, Fernandes R. Biochemistry of adipose tissue: an endocrine organ. Arch Med Sci. 2013;9(2):191–200. doi: https://doi.org/10.5114/aoms.2013.33181
6. Rezaee F, Dashty M. Role of adipose tissue in metabolic system disorders. J Diabetes Metab. 2013;01(S13):1–9. doi: https://doi.org/10.4172/2155-6156.S13-008
7. Gjermeni E, Kirstein AS, Kolbig F, Kirchhof M, Bundalian L, Katzmann JL, *et al.* Obesity–an update on the basic pathophysiology and review of recent therapeutic advances. Biomolecules. 2021;11(10):1426. doi: https://doi.org/10.3390/biom11101426
8. Ghoch ME, Fakhoury, R. Challenges and new directions in obesity management: lifestyle modification programmes, pharmacotherapy and bariatric surgery. J Popul Ther Clin Pharmacol. 2019;26(2):e1–e4. doi: https://doi.org/10.15586/jptcp.v26i2.599
9. Ross R. Commentary the challenge of obesity treatment : avoiding weight regain. CMAJ. 2009;180(10):997–8. doi: https://doi.org/10.1503/cmaj.090427
10. Muller TD, Blüher M, Tschöp MH, Dimarchi RD. Anti-obesity drug discovery: advances and challenges. Nat Rev Drug Discov. 2022;21:201–23. doi: https://doi.org/10.1038/s41573-021-00337-8
11. Choe SS, Huh JY, Hwang IJ, Kim JI, Kim JB. Adipose tissue remodeling: Its role in energy metabolism and metabolic disorders. Front Endocrinol (Lausanne). 2016;7:1–16. doi: https://doi.org/10.3389/fendo.2016.00030
12. Hammarstedt A, Gogg S, Hedjazifar S, Nerstedt A, Smith U. Impaired adipogenesis and dysfunctional adipose tissue in human hypertrophic obesity. Physiol Rev. 2018;98(4):1911–41. doi: https://doi.org/10.1152/physrev.00034.2017
13. Kuryłowicz A, Puzianowska-Kuźnicka M. Induction of adipose tissue browning as a strategy to combat obesity. Int J Mol Sci. 2020;21(17):1–28. doi: https://doi.org/10.3390/ijms21176241
14. McNeill BT, Suchacki KJ, Stimson RH. Human brown adipose tissue as a therapeutic target: warming up or cooling down? Eur J Endocrinol. 2021;184(6):R243–59. doi: https://doi.org/10.1530/EJE-20-1439
15. Machado SA, Pasquarelli-do-Nascimento G, da Silva DSS, Farias GR, de Oliveira Santos I, Baptista LB, *et al.* Browning of the white adipose tissue regulation: new insights into nutritional and metabolic relevance in health and diseases. Nutr Metab. 2022;19(1):1–27. doi: https://doi.org/10.1186/s12986-022-00694-0
16. Lee MK, Lee B, Kim CY. Natural extracts that stimulate adipocyte browning and their underlying mechanisms. Antioxidants. 2021;10(2):1–17. doi: https://doi.org/10.3390/antiox10020308
17. Ku HC, Chan TY, Chung JF, Kao YH, Cheng CF. The ATF3 inducer protects against diet-induced obesity via suppressing adipocyte adipogenesis and promoting lipolysis and browning. Biomed Pharmacother. 2022;145:112440. doi: https://doi.org/10.1016/j.biopha.2021.112440
18. Lin C, Chen J, Hu M, Zheng W, Song Z, Qin H. Sesamol promotes browning of white adipocytes to ameliorate obesity by inducing mitochondrial biogenesis and inhibition mitophagy via β3-AR/PKA signaling pathway. Food Nutr Res. 2021;65:7577. doi: https:// doi.org/10.29219/fnr.v65.7577
19. Wang H, Yu L, Wang J, Zhang Y, Xu M, Lv C, *et al.* SLC35D3 promotes white adipose tissue browning to ameliorate obesity by NOTCH signaling. Nat Commun. 2023;14(1): 7643. doi: https://doi.org/10.1038/s41467-023-43418-5
20. El Hadi H, Di Vincenzo A, Vettor R, Rossato M. Food ingredients involved in white to brown adipose tissue conversion in calorie burning. Front. Physiol. 2019;9:1954. doi: https://doi.org/10.3389/fphys.2018.01954
21. Suchacki KJ, Stimson RH, Al-Mrabeh A. Nutritional regulation of human brown adipose tissue. Nutrients. 2021;13:1748. doi: https://doi.org/10.3390/nu13061748
22. Vargas-Castillo A, Fuentes-Romero R, Rodriguez-Lopez LA, Torres N, Tovar AR. Understanding the biology of thermogenic fat: Is browning a new approach to the treatment of obesity? Arch Med Res. 2017;48(5):401–13. doi: https://doi.org/10.1016/j.arcmed.2017.10.002
23. Borah AK, Sharma P, Singh A, Kalita KJ, Saha S, Chandra Borah J. Adipose and non-adipose perspectives of plant-derived natural compounds for mitigation of obesity. J Ethnopharmacol. 2021;280:114410. doi: https://doi.org/10.1016/j.jep.2021.114410

24. Wang S, Pan MH, Hung WL, Tung YC, Ho CT. From white to beige adipocytes: therapeutic potential of dietary molecules against obesity and their molecular mechanisms. Food Function. 2019;10:1263–79. doi: https://doi.org/10.1039/c8fo02154f
25. Cheng L, Wang J, Dai H, Duan Y, An Y, Shi L, *et al.* Brown and beige adipose tissue: a novel therapeutic strategy for obesity and type 2 diabetes mellitus. Adipocyte. 2021;10(1):48–65. doi: https://doi.org/10.1080/21623945.2020.1870060
26. Kassahun T, Girma B, Kumer Joshi R, Sisay B, Tesema S, Teka F, *et al.* Ethnobotany, traditional use, phytochemistry and pharmacology of *Cymbopogon citratus*: review article. Int J Herb Med. 2020;8(4):80–7. https://www.florajournal.com/archives/2020/vol8issue4/PartB/7-5-52-470.pdf
27. Bharti SK, Kumar A, Prakash O, Sharma NK, Krishnan S, Gupta AK. Essential oil of *Cymbopogon citratus* against diabetes: validation by *in vivo* experiments and computational studies. Open Access Sci Rep. 2013;2(3):1–9. doi: https://dx.doi.org/10.4172/1948-593X.100009
28. Ajayi EO, Sadimenko AP, Afolayan AJ. GC-MS evaluation of *Cymbopogon citratus* (DC) Stapf oil obtained using modified hydro-distillation and microwave extraction methods. Food Chem. 2016;209:262–6. doi: https://doi.org/10.1016/j.foodchem.2016.04.071
29. Katsukawa M, Nakata R, Takizawa Y, Hori K, Saori T, Hiroyasu I. Citral, a component of lemongrass oil, activates PPARα and γ and suppresses COX-2 expression. Biochimica et Biophysica Acta. 2010;1801:1214–20. doi: https://doi.org/10.1016/j.bbalip.2010.07.004
30. Shen Y, Sun Z, Guo X. Citral inhibits lipopolysaccharide-induced acute lung injury by activating PPAR-γ. Eur J Pharmacol. 2015;747:45–51. doi: https://dx.doi.org/10.1016/j.ejphar.2014.09.040
31. Wang L, Waltenberger B, Pferschy-Wenzig EM, Blunder M, Liu X, Malainer C, *et al.* Natural product agonists of peroxisome proliferator-activated receptor gamma (PPARγ): a review. Biochem Pharmacol. 2014;92(1):73–89. doi: https://dx.doi.org/10.1016/j.bcp.2014.07.018
32. Ohno H, Shinoda K, Spiegelman BM, Kajimura S. PPARγ agonists induce a white-to-brown fat conversion through stabilization of PRDM16 protein. Cell Metab. 2012;15(3):395–404. doi: https://dx.doi.org/10.1016/j.cmet.2012.01.019
33. Kajimura S. Promoting brown and beige adipocyte biogenesis through the PRDM16 pathway. Int J Obes Suppl. 2015;5(S1):S11–4. doi: https://dx.doi.org/10.1038/ijosup.2015.4
34. Jo YS, Ju SM, Hwang KH, Kim KS, Kim MS, Jeon BH. Inhibitory effect of *Cymbopogon Citratus* ethanol extracts on adipogenesis in 3T3-L1 preadipocytes. J Physiol Pathol Korean Med. 2019;33(1):17–24. doi: https://doi.org/10.15188/kjopp.2019.02.33.1.17
35. Xiao B, Sanders MJ, Carmena D, Bright NJ, Haire LF, Underwood E, *et al.* Structural basis of AMPK regulation by small molecule activators. Nat Commun. 2013;4:3017. doi: https://doi.org/10.1038/ncomms4017
36. Gampe RT, Montana VG, Lambert MH, Miller AB, Bledsoe RK, Milburn M V, *et al.* Asymmetry in the PPARgamma/RXRalpha crystal structure reveals the molecular basis of heterodimerization among nuclear receptors. Mol Cell. 2000;5(3):545–55. doi: https://doi.org/10.1016/s1097-2765(00)80448-7
37. Rohman MS, Lukitasari M, Kholis MN, Wahyuni NA, Chandra BR, Hermanto FE, *et al.* Combination of decaffeinated green coffee and decaffeinated green tea ameliorates cardiomyopathy through cardiotrophin-1-dependent expression regulation in a metabolic syndrome rat model: a proposed mechanism. Beni-Suef Univ J Basic Appl Sci. 2023;9;12(1):53. doi: https://doi.org/10.1186/s43088-023-00381-w
38. Widyananda MH, Wicaksono ST, Rahmawati K, Puspitarini S, Ulfa SM, Jatmiko YD, *et al.* A potential anticancer mechanism of finger root (*Boesenbergia rotunda*) extracts against a breast cancer cell line. Erickson KL, editor. Scientifica (Cairo). 2022 Oct 31;2022:9130252. doi: https://doi.org/10.1155%2F2022%2F9130252
39. Ekpenyong C. *Cymbopogon citratus* Stapf (DC) extract ameliorates atherogenic cardiovascular risk in diabetes-induced dyslipidemia in rats. Br J Med Med Res. 2014;4(28):4695–709. doi: https://doi.org/10.9734/BJMMR/2014/11262
40. Andrade EHA, Zoghbi M das GB, Lima M da P. Chemical composition of the essential oils of *Cymbopogon citratus* (dc.) stapf cultivated in north of brazil. J Essent Oil-Bearing Plants. 2009;12(1):41–5. doi: https://dx.doi.org/10.1080/0972060X.2014.935075
41. Mohamed Hanaa AR, Sallam YI, El-Leithy AS, Aly SE. Lemongrass (*Cymbopogon citratus*) essential oil as affected by drying methods. Ann Agric Sci. 2012;57(2):113–6. doi: https://dx.doi.org/10.1016/j.aoas.2012.08.004
42. Tajidin NE. Chemical composition and citral content in lemongrass (*Cymbopogon citratus*) essential oil at three maturity stages. Afr J Biotechnol. 2012;11(11):2685–93. doi: https://dx.doi.org/10.5897/AJB11.2939
43. da Silva TLM, da Rosa GI, dos Santos MAL, Graf SL, de Noronha Sales Maia BHL, Beltrame FL, *et al*. Lemongrass essential oil (*Cymbopogon citratus* (DC) Stapf.) seasonal evaluation and microencapsulation by spray-drying. Brazil Arch Biol Technol. 2023;66(spe):1–12. doi: https://dx.doi.org/10.1590/1678-4324-ssbfar-2023230016
44. Silva GBVU D, Rasp S, Sku S. Comparison of essential oil content and composition of different parts of *Cymbopogon citratus* (DC.) Stapf (Poaceae) grown in Sri Lanka "Comparison of essential oil content and composition of different parts of *Cymbopogon citratus* (DC.) Stapf (Poaceae) Gro. World J Agric Res. 2020;8(1):1–5. doi: https://dx.doi.org/ 10.12691/wjar-8-1-1
45. Trang DT, Hoang TK Van, Nguyen TTM, Van Cuong P, Dang NH, Dang HD, *et al.* Essential oils of lemongrass (*Cymbopogon citratus* Stapf) induces apoptosis and cell cycle arrest in A549 lung cancer cells. Biomed Res Int. 2020;2020:5924856. doi: https://doi.org/10.1155/2020/5924856
46. Olayemi RF. Comparative study of root, stalk and leaf essential oils of *Cymbopogon citratus* (lemon grass). ChemSearch J. 2017;8(1):20–8. doi: https://dx.doi.org/10.4314/csj.v8i1.3
47. Nguyen NT, Nguyen TH, Pham TNH, Huy NT, Bay M Van, Pham MQ, *et al*. Autodock Vina adopts more accurate binding poses but Autodock4 forms better binding affinity. J Chem Inf Model. 2020;60(1):204–11. doi: https://doi.org/10.1021/acs.jcim.9b00778
48. Pantsar T, Poso A. Binding affinity via docking: fact and fiction. Molecules. 2018;23(8):1899. doi: https://doi.org/10.3390/molecules23081899
49. Susilo A, Cahyati M, Pranowo D, Nurjannah, Masyithoh D, Awwaly KU Al, *et al.* Simulasi molekuler pada bidang pangan fungsional, prinsip dasar dan tutorial. Malang, Indonesia: UB Press; 2023. p 148.
50. Patil R, Das S, Stanley A, Yadav L, Sudhakar A, Varma AK. Optimized hydrophobic interactions and hydrogen bonding at the target-ligand interface leads the pathways of drug-designing. PLoS One. 2010. 8;5(8):e12029. doi: https://doi.org/10.1371/journal.pone.0012029
51. Balusamy SR, Perumalsamy H, Veerappan K, Huq MA, Rajeshkumar S, Lakshmi T *et al.* Citral induced apoptosis through modulation of key genes involved in fatty acid biosynthesis in human prostate cancer cells: *in silico* and *in vitro* study. BioMed Res Int. 2020;2020:6040727. doi: https://doi.org/10.1155/2020/6040727
52. Timm KN, Tyler DJ. The role of AMPK activation for cardioprotection in doxorubicin-induced cardiotoxicity. Cardiovasc Drugs Ther. 2020;34(2):255–69. doi: https://doi.org/10.1007/s10557-020-06941-x
53. Tarasiuk O, Miceli M, Di Domizio A, Nicolini G. AMPK and diseases: state of the art regulation by AMPK-targeting molecules. Biology (Basel). 2022;8;11(7):1041. https://www.mdpi.com/2079-7737/11/7/1041.
54. Wu C, Guo Y, Su Y, Zhang X, Luan H, Zhang X, *et al.* Cordycepin activates AMP-activated protein kinase (AMPK) via interaction with

the γ1 subunit. J Cell Mol Med. 2014;18(2):293–304. doi: https://doi.org/10.1111/jcmm.12187
55. Bonora M, Patergnani S, Rimessi A, De Marchi E, Suski JM, Bononi A, *et al.* ATP synthesis and storage. Purinergic Signal. 2012;8(3):343–57. doi: https://doi.org/10.1007/s11302-012-9305-8
56. Fediuc S, Gaidhu MP, Ceddia RB. Regulation of AMP-activated protein kinase and acetyl-CoA carboxylase phosphorylation by palmitate in skeletal muscle cells. J Lipid Res. 2006;47(2):412–20. doi: https://doi.org/10.1194/jlr.m500438-jlr200
57. Desjardins EM, Steinberg GR. Emerging role of AMPK in brown and beige adipose tissue (BAT): implications for obesity, insulin resistance, and type 2 diabetes. Curr Diab Rep. 2018;18(10):80. doi: https://doi.org/10.1007/s11892-018-1049-6
58. Mottillo EP, Desjardins EM, Crane JD, Smith BK, Green AE, Ducommun S, *et al.* Lack of adipocyte AMPK exacerbates insulin resistance and hepatic steatosis through brown and beige adipose tissue function. Cell Metab. 2016;24(1):118–29. doi: https://doi.org/10.1016%2Fj.cmet.2016.06.006
59. Van Der Vaart JI, Boon MR, Houtkooper RH. The role of AMPK signaling in brown adipose tissue activation. Cells. 2021;9;10(5):1122. doi: https://doi.org/10.3390%2Fcells10051122
60. Edvardsson U, Bergström M, Alexandersson M, Bamberg K, Ljung B, Dahllöf B. Rosiglitazone (BRL49653), a PPARgamma-selective agonist, causes peroxisome proliferator-like liver effects in obese mice. J Lipid Res. 1999;40(7):1177–84.
61. Al Sharif M, Tsakovska I, Alov P, Vitcheva V, Diukendjieva A, Pajeva I. Molecular modeling approach to study the PPARγ–ligand interactions. Nuclear Receptors. New York, NY: Springer New York; 2019. pp 261–89. doi: https://doi.org/10.1007/978-1-4939-9195-2_22
62. Tsakovska I, Al Sharif M, Alov P, Diukendjieva A, Fioravanzo E, Cronin MTD, *et al.* Molecular modelling study of the PPARγ receptor in relation to the mode of action/adverse outcome pathway framework for liver steatosis. Int J Mol Sci. 2014;15(5):7651–66. doi: https://dx.doi.org/10.3390/ijms15057651
63. Hansson B, Rippe C, Kotowska D, Wasserstrom S, Säll J, Göransson O, *et al.* Rosiglitazone drives cavin-2/SDPR expression in adipocytes in a CEBPα-dependent manner. PLoS One. 2017;12(3):e0173412. doi: https://doi.org/10.1371%2Fjournal.pone.0173412
64. Siersbaek R, Nielsen R, Mandrup S. PPARgamma in adipocyte differentiation and metabolism--novel insights from genome-wide studies. FEBS Lett. 2010;584(15):3242–9. doi: https://doi.org/10.1016/j.febslet.2010.06.010
65. Madsen MS, Siersbæk R, Boergesen M, Nielsen R, Mandrup S. Peroxisome proliferator-activated receptor γ and C/EBPα synergistically activate key metabolic adipocyte genes by assisted loading. Mol Cell Biol. 2014;34(6):939–54. doi: https://doi.org/10.1128%2FMCB.01344-13
66. Mu Q, Fang X, Li X, Zhao D, Mo F, Jiang G, *et al.* Ginsenoside Rb1 promotes browning through regulation of PPARγ in 3T3-L1 adipocytes. Biochem Biophys Res Commun. 2015;466(3):530–5. doi: https://doi.org/10.1016/j.bbrc.2015.09.064
67. Fayyad AM, Khan AA, Abdallah SH, Alomran SS, Bajou K, Khattak MNK. Rosiglitazone enhances browning adipocytes in association with MAPK and PI3-K pathways during the differentiation of telomerase-transformed mesenchymal stromal cells into adipocytes. Int J Mol Sci. 2019;20(7):1618. doi: https://doi.org/10.3390/ijms20071618
68. Widyananda MH, Fatchiyah F, Muflikhah L, Widodo N. Computational examination to reveal Kaempferol as the most potent active compound from *Euphorbia hirta* against breast cancer by targeting AKT1 and ERα. Egypt J Basic Appl Sci. 2023;10(1):753–67. doi: https://doi.org/10.1080/2314808X.2023.2272385.
69. Wargasetia TL, Ratnawati H, Widodo N, Widyananda MH. Bioinformatics study of sea cucumber peptides as antibreast cancer through inhibiting the activity of overexpressed protein (EGFR, PI3K, AKT1, and CDK4). Cancer Inform. 2021;20:117693512110318. doi: https://journals.sagepub.com/doi/10.1177/11769351211031864
70. Suryono S, Rohman MS, Widjajanto E, Prayitnaningsih S, Wihastuti TA. Colchicine as potential inhibitor targeting MMP-9, NOX2 and TGF-β1 in myocardial infarction: a combination of docking and molecular dynamic simulation study. J Biomol Struct Dyn. 2023;41(21):12214–24. doi: https://doi.org/10.1080/07391102.2023.2166590

How to cite this article:
Mashitah MW, Widodo N, Permatasari N, Rudijanto A. The potential of citral isomers from lemongrass (*Cymbopogon citratus*) essential oil as WAT browning agents in obesity by activating AMPK and PPARγ: An *in silico* approach. J Appl Pharm Sci. 2025;15(04):116–128.